This article has been accepted for publication in a future issue of this journal, but has not been fully edited. Content may change prior to final publication. Citation information: DOI 10.1109/LAWP.2021.3076673, IEEE Antennas and Wireless Propagation Letters

High-Gain Compact Circularly Polarized X-Band Superstrate Antenna for CubeSat Applications

L. Leszkowska, M. Rzymowski, *Member, IEEE*, K. Nyka, *Senior Member, IEEE* and L. Kulas, *Senior Member, IEEE*

***Abstract*— In this letter, a concept of high-gain circularly polarized X-band antenna employing a partially reflecting surface (PRS) has been presented. In the initial antenna analysis, the influence of parasitic elements size in the PRS structure on antenna radiation pattern parameters has been investigated and the optimal arrangement of the elements has been identified. The proposed antenna provides wide bandwidth of return loss above 10 dB of 20% (8-9.8 GHz) and circular polarization in a frequency range 8.35-8.95 GHz. The final design is compact (62 × 62 × 22.2 mm) and lightweight (29.7 g), which makes it suitable for use in CubeSat X-band communication systems but also drone and high-altitude pseudo-satellite (HAPS) applications.**

***Index Terms*— partially reflecting surface (PRS), high-gain antenna, circular polarization, microstrip antenna.**

I. Introduction

Long range communication between such objects as unmanned aerial vehicles (UAVs), high-altitude pseudo-satellites (HAPS) or satellite platforms and ground stations can be a complementary way for terrestrial infrastructure of wireless sensor networks especially when one is interested in monitoring large areas, e.g. in smart farming applications [1]-[4]. Such applications can provide huge surface coverage, especially when satellites operate within larger formations or constellations.

Small satellites, e.g. based on the CubeSat standard, are particularly useful in creating satellite constellations. The growing popularity of the CubeSat standard has been observed in recent years due to the real need for commercial applications for small, lightweight and inexpensive satellites [5], [6]. CubeSat standard is based on a structure with fixed dimensions of 100 mm × 100 mm × 100 mm, which constitutes a single 1U module and a light weight not exceeding 1.3 kg per module. These modules can be combined, however, the structure of the Poly Picosatellite Orbital Deployer (P-POD), which is a container that carries the satellite into space as a rocket load, imposes limitation on maximum CubeSat weight. In result, apart from a need for high gain and wideband operation of antennas, small size, low weight, and high efficiency have to be considered for practical space applications [7], [8].

The main task of communication modules installed on small satellites is transmission of high amount of data obtained from remote sensing in research missions, high-resolution surface imaging or tracking [6]. Efficient and good quality downlink communication can be provided by antennas with circular polarization (CP) prevents from polarization mismatch due to changes in the relative orientation of transmitting antenna towards receiving antenna. What is also particularly meaningful in the context of satellite communication, CP makes the link resistant to impact of Faraday effect. Relatively small dimensions and wide bandwidth necessary for the transmission of large amounts of data can be achieved for antenna designed for the X band [9]-[12]. Microstrip antennas meet the assumption in small satellites as to their low cost, weight and size, however, their disadvantage is low gain. In [9], a patch antenna with printed parasitic dipoles for satellite applications using isoflux radiation pattern has been reported. The gain of the antenna is about 6 dBi and total dimension of the antenna is 83 mm × 83 mm × 15 mm. The common method of increasing gain is to create arrays but, as a consequence, losses in the feeding network usually cause decreased efficiency of such antennas [10], [12].

The gain of a single-patch antenna can be effectively improved by placing an additional layer above the patch [13]-[18]. The improvement of the antenna parameters can be realized by applying a set of holes in the superstrate layer [14], [15] or by placing an array of printed parasitic patches with equal sizes and constant interelement spacing [13], [16]. In [17], varied elements, optimally selected in number and size of particular passive elements, were used to optimize gain, side-lobe level (SLL) and beamwidth of a linearly polarized (LP) superstrate antenna. In result, a 5.9 GHz LP superstrate

This work was supported in part by the AFARCLOUD Project through the ECSEL Joint Undertaking (JU) under grant agreement No 783221 and in part by the European Union's Horizon 2020 research and innovation programme and Austria, Belgium, Czech Republic, Finland, Germany, Greece, Italy, Latvia, Norway, Poland, Portugal, Spain, Sweden.

The authors would like to thank the Academic Computer Centre in Gdansk, Poland (TASK) where all the calculations were carried out.

The authors are with the Department of Microwave and Antenna Engineering, Faculty of Electronics, Telecommunications and Informatics, Gdansk University of Technology, Narutowicza 11/12, 80-233 Gdansk, Poland (e-mail: luiza.leszkowska@pg.edu.pl, mateusz.rzymowski@pg.edu.pl krzysztof.nyka@pg.edu.pl, lukasz.kulas@pg.edu.pl).

This article has been accepted for publication in a future issue of this journal, but has not been fully edited. Content may change prior to final publication. Citation information: DOI 10.1109/LAWP.2021.3076673, IEEE Antennas and Wireless Propagation Letters

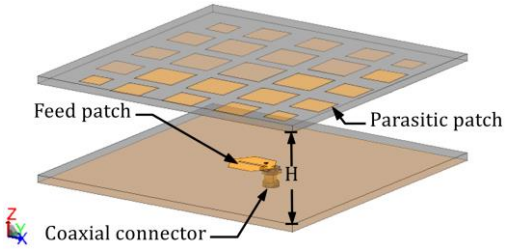

Fig. 1. Geometry of the antenna with superstrate layer (side view), in which parasitic patches are facing the active patch.

antenna having only a 5 × 5 array of square patches provided a gain of 18.0 dB and SLL equal -18.4 dB. An interesting solution is a transformation of polarization from LP excitation source to CP in Fabry-Perot Cavity (FPC) antenna, utilizing a high impedance surface (HIS) which allows for independent control of reflection and transmission field components inside the cavity [18]. However, this approach suffers from difficulties in obtaining AR below 3 dB and return loss above 10 dB simultaneously in the wide common bandwidth.

In this paper, we have adapted the method of optimal selection of square elements for the superstrate layer introduced in [17] for LP antennas to design and manufacture a left-handed circularly polarized (LHCP) superstrate antenna for CubeSat X-band communication. The proposed antenna has reduced cross-polarization radiation and smaller overall dimension compared to the previous CP superstrate antenna designs [13], [19]. The result of this work is a compact lightweight antenna that was fabricated and measured. The antenna exhibits gain over 14 dBic and Axial Ratio (AR) less than 3 dB bandwidth of about 6%.

II. Antenna Concept and Design

The way the proposed antenna radiates is based on the operating principle of FPC [14]. In the presented structure, the cavity is formed between the ground plane and the array of passive metal elements printed on the dielectric layer which acts as partially reflecting surface (PRS), as it is shown in Fig. 1. The wave exited from the active element reflects at PRS, which can cause constructive interference and result in focusing of the beam radiated from the active patch. For the maximum gain improvement, the distance between PRS and the ground plane should be about half the free-space wavelength [14]. The design procedure of the antenna relies solely on the full-wave electromagnetic simulations in Altair FEKO and thus does not involve any separate considerations for the leaky-wave modes in FPC antennas.

A. Feeding element design

In the proposed concept, a CP single-feed hexagonal-shaped patch with a slot is used as a source element inside the cavity. The patch is printed on RO3003 substrate with thickness of 1.52 mm, permittivity of 3.0 and loss tangent of 0.001. The patch is fed from 50 Ω line through a coaxial probe with the feed point shifted by P_x and P_y from the center of the patch in x- and y-axis, respectively. All dimensions of the patch are shown in Fig. 2. This type of radiating patch was chosen after designing several types of CP patch antennas that were tuned after the

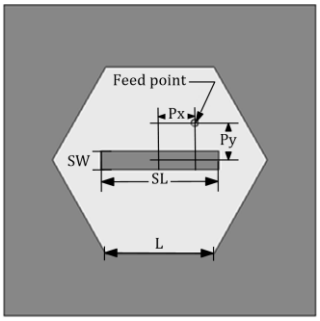

Fig. 2. Geometry of the designed microstrip patch antenna used as feeding element with left hand circular polarization (L=5.34 mm, S_L=6.5 mm, S_W=0.54 mm, P_x=1.9 mm, P_y=2.05 mm).

TABLE I
Overview of the Investigated Feeding Elements

Type	circular patch with a slot	hexagonal patch with a slot	circular patch with a stub	rectangular patch with corners' truncation
Gain [dBic]	4.57	4.57	4.56	4.56
Size (the largest dimension)	9.8 mm (diameter)	10.7 mm (longer diagonal)	13 mm (longer diagonal)	13 mm (diameter with stub length)
HPBW [˚] ϕ=0˚/ ϕ=90˚	110.5/111.2	110.9/111.2	108.7/112.1	111.6/106.1
Efficiency [%]	98.1	98.1	98.2	97.9

superstrate layer is added. In the study on proposed antenna design, we focused on the antennas where CP is provided by various means such as perturbations in the form of a slot or stub in circular or hexagonal patch and diagonal corners truncation in rectangular patch. Due to the same feeding method and similar dimensions, each of the investigated patches, when employed as a primary radiating element in the antenna with a superstrate layer, gives similar bandwidth and gain. Besides these two key factors, another desirable property is even distribution of the fields reaching the superstrate layer. With this respect, small size of the element and the symmetry of the patch are also important. A brief summary of basic characteristics of the investigated radiating patches is shown in Table I.

B. Superstrate design

The superstrate layer for the proposed antenna is designed in such a way as to achieve highest gain and wide AR parameter less than 3 dB bandwidth. For this purpose, RO3003 substrate with thickness of 1.52 mm is placed at a distance H above the ground plane. In order to increase the reflection coefficient of this structure, an array of metal parasitic patches is arranged on the bottom side of the layer [17]. Because uniform size of superstrate elements proposed in [13] cause high cross-polarization radiation [19], we have used square shape of passive elements that are distributed in a 5 × 5 rectangular grid symmetrical with respect to the x- and y-axes, which was proposed as optimal for a LP superstrate antenna [17]. The geometry of the proposed superstrate layer is presented in Fig. 3 where the letters indicate elements having the same size.

The proposed design process relies on the observation, that

This article has been accepted for publication in a future issue of this journal, but has not been fully edited. Content may change prior to final publication. Citation information: DOI 10.1109/LAWP.2021.3076673, IEEE Antennas and Wireless Propagation Letters

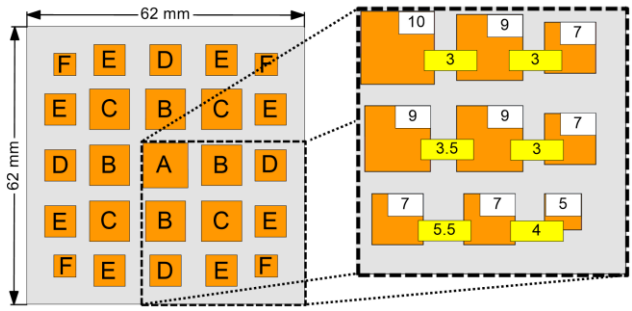

Fig. 3. Geometry of the proposed superstrate layer with dimensions (in millimeters). In the white boxes, sizes of square patches are presented, while in the yellow boxes distances between them on the dielectric layer are shown.

parasitic elements placed further from the radiating patch are smaller than the element located centrally [17]. Due to the fact that the central element in the array has the largest influence on the antenna parameters, to compensate the phase variation, the elements size optimization has been carried out starting from the central element (labeled A in Fig. 3). The next optimization step involved four elements (labeled B) added to the superstrate layer and their size and placement with respect to the central element has been optimized. This procedure was caried out until the last set of elements (labeled F) was reached. In each step, optimization involved the following antenna parameters: gain, AR, cross-polarization level, SLL and beamwidth. Since AR value is particularly vulnerable to any modifications in the antenna, it was necessary to slightly adjust the dimensions of the radiating patch and the air gap between the radiating patch and the superstrate layer in the final design. Although the proposed procedure is sufficiently effective for small structures to be fit in CubeSats, it may slow down for larger PRS sizes.

III. Numerical Results

In all simulations, the parameters of the proposed antenna with varied size of the parasitic patches (PPs) placed within the superstrate layer were compared with the results obtained for a reference design having PPs of the same size arranged in a 5 × 5 array with a patch size equal to 10 mm, 9 mm, 8 mm, 7 mm, 6 mm, and equal spacing between PPs set to 3 mm in all cases.

TABLE II
Specification of the Antenna with Different PRS Configurations

PP size [mm]	10	9	8	7	6	varied
S11 (-10 dB) [MHz]	1346	1303	1341	1344	1365	1381
AR 3dB [MHz]	-	450	468	383	-	600
Peak gain [dBic]	13.7	13.6	13.4	13.4	12.5	14.5
HPBW [°] @8.6GHz	26.7	28.3	30.1	31.7	34.0	29.3
Efficiency [%]	95	95	96	95	96	95
SLL [dB] @8.6GHz	-9.7	-11.5	-13.0	-15.5	-15.7	-14.8
SLL < -10dB [MHz]	300	900	1100	1100	1500	900
Cross-pol. level [dB] @8.6GHz	-15.2	-19.3	-25.8	-19.7	-14.2	-27.3
Cross-pol. < -15dB [MHz]	160	460	480	400	-	610
Front-to-back ratio (RHC) @8.6GHz [dB]	25.6	32.8	43.3	35.0	31.2	39.8

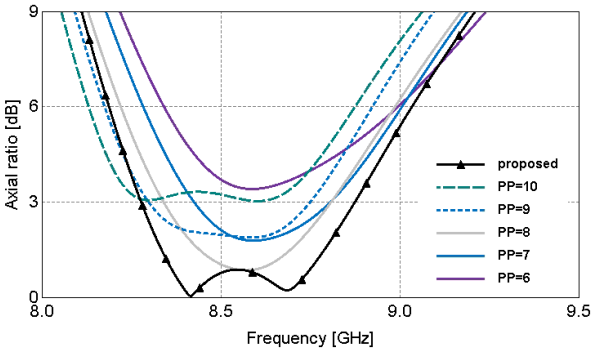

Fig. 4. Simulated axial ratio of the antenna with different PRS configurations (see test for explanations)

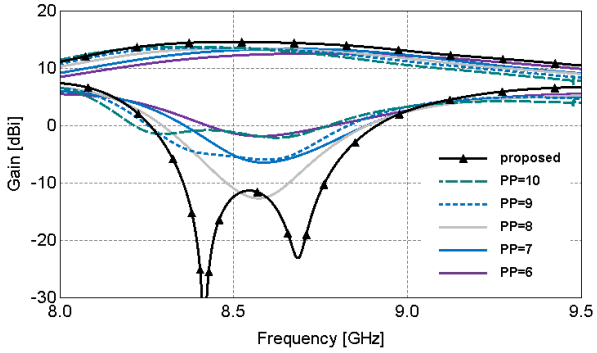

Fig. 5. Simulated LHCP and RHCP radiation of the antenna with different PRS configurations (see test for explanations)

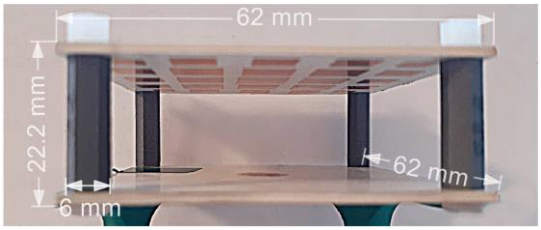

Fig. 6. Fabricated X-band antenna with the proposed superstrate layer.

The simulation results, which were obtained using Altair FEKO, are summarized in detail in Table II and are presented in Fig. 4, and Fig. 5. It can easily be noticed that all the considered PRS configurations have similar S11 bandwidth, which is wider than 15% in every case, efficiency, and high gain above 12 dBic. However, the biggest advantage of using varied size of the PPs placed within the superstrate lies in high AR 3-dB bandwidth, and cross-polarization radiation levels below -25 dB in a wide frequency range, which can also be seen in Fig. 5.

IV. Measurements

The optimized design of the proposed PRS antenna was fabricated and its prototype is presented in Fig. 6. To ensure the separation between the feeding element and the superstrate layer, four 3D-printed plastic spacers were used to provide the exact distance. The antenna measurements were conducted in our 11.9 m × 5.6 m × 6.0 m anechoic chamber and are shown in Fig. 7 – Fig. 10.

This article has been accepted for publication in a future issue of this journal, but has not been fully edited. Content may change prior to final publication. Citation information: DOI 10.1109/LAWP.2021.3076673, IEEE Antennas and Wireless Propagation Letters

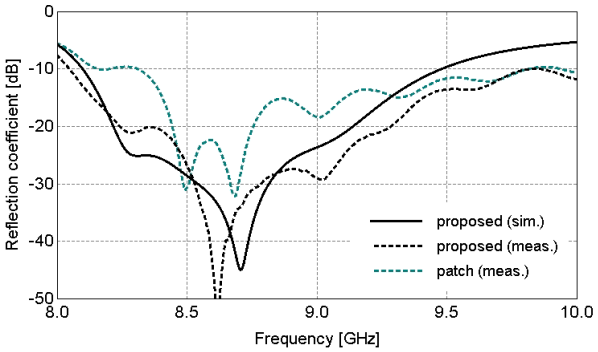

Fig. 7. Measured reflection coefficient of the proposed antenna compared to the initial antenna without additional layer

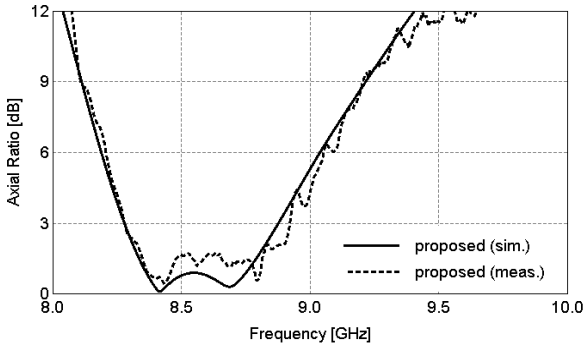

Fig. 8. Measured axial ratio of the proposed antenna.

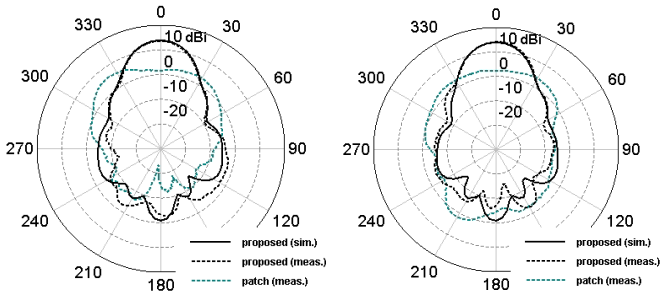

(a) (b)

Fig. 9. Measured radiation patterns of the antenna with different PRS configurations at 8.6 GHz: (a) Φ = 0° plane (b) Φ = 90° plane

As it can be seen in Fig. 7, the proposed antenna is well matched in the entire bandwidth. Similarly, AR results presented in Fig. 8 match those from numerical simulations and in the frequency range of axial ratio below 3 dB, the reflection coefficient is maintained below -20 dB. Radiation patterns of the proposed antenna visible in Fig. 9 show good agreement with numerical simulations and illustrate the beam narrowing effect when the proposed superstrate layer is applied. By placing the additional reflecting layer, the antenna beamwidth changes from 105˚ to 30˚. In consequence, the proposed antenna can provide LHCP in the entire bandwidth with acceptable cross-polarization levels, shown in Fig. 10. A summarizing performance comparison between the proposed antenna and the other fabricated and measured compact antennas reported in the literature is presented in Table III. The comparison shows that the proposed antenna for X-band communication outperforms other designs if the collection of all the parameters important for CubeSat applications, including S11 bandwidth, SLL, gain, cross-polarization level, and size, is considered.

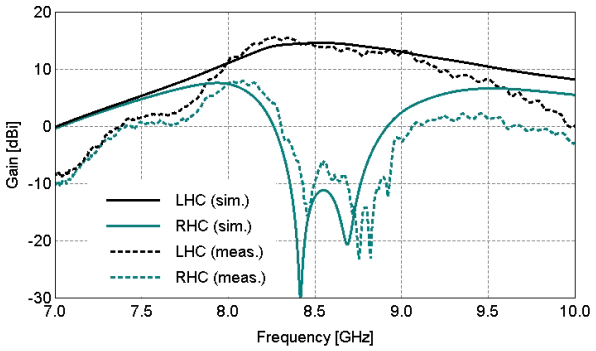

Fig. 10. Measured co- and cross-polarization level of the proposed antenna

TABLE III
COMPARISON OF CHARACTERISTICS OF THE PROPOSED ANTENNA WITH AVAILABLE FABRICATED AND MEASURED SOLUTIONS

Ref.	Common bandwidth of AR < 3dB and S11 < -10dB [%]	Pol.	Peak gain [dBi]	SLL [dB]	Cross-pol. level [dB]	Overall size [mm^3]
[9]	~4.8 (from 8.0 to 8.4 GHz)	RHCP	6	-	-22	83 × 83 × 15
[13]	2.44 (from 8.1 to 8.3 GHz)	CP	20.5*	~-13*	-24*	170 × 170 × 21.5
[17]	~2.6 (from 5.725 to 5.875 GHz)**	linear	18	-18.4	-22.2	115 × 115 × 30
[18]	~2 (from 14.9 to 15.2 GHz)	RHCP	19.1	-20	-20	137.5 × 137.5 × 10.2
[19]	4.1* (from 8.6 to 8.95 GHz)	RHCP	16.3*	-18*	-16.4	68.5 × 68.5 × 21
Proposed	7 (from 8.28 to 8.88 GHz)	LHCP	14.6	-14.8	-27.3	62 × 62 × 22.2

** only simulated results are available; ** bandwidth of S11 < -10 dB only*

V. CONCLUSIONS

In this article, the design and realization of a compact high-gain and wide AR bandwidth superstrate CP antenna for X-band aerospace communication, has been proposed. The antenna has a simple mechanical structure, which consist of an active feeding element and a superstrate layer containing passive patches, compact overall size of 62 mm × 62 mm × 22.2 mm (1.78λ × 1.78λ × 0.64λ) and low weight of 29.7 g that makes it applicable to CubeSat missions. By optimizing size of the passive elements within the superstrate layer, an appropriate phase distribution can be reached that, in turn, increases gain, widens AR 3-dB bandwidth, and improves cross-polarization suppression in a wide frequency bandwidth. In result, the proposed antenna can also be used in systems in which the two orthogonal antennas are used to increase the bandwidth or for frequency reuse within the same satellite.

REFERENCES

[1] I. Bhakta, S. Phadikar, K. Majumder, "State-of-the-art technologies in precision agriculture: a systematic review", *Journal of the Science of Food and Agriculture*, vol. 99, pp. 4878, 2019.

[2] S. Candiago, F. Remondino, M. De Giglio, M. Dubbini and M. Gattelli, "Evaluating Multispectral Images and Vegetation Indices for Precision Farming Applications from UAV Images", *Remote Sens.*, vol. 7, no. 4, pp. 4026, 2015.

[3] T. Adão et al., "Hyperspectral imaging: A review on UAV-based sensors data processing and applications for agriculture and forestry", *Remote Sens.*, vol. 9, no. 11, pp. 1110, 2017.

[4] P. Horstrand, R. Guerra, A. Rodríguez, M. Díaz, S. López and J. F. López, "A UAV Platform Based on a Hyperspectral Sensor for Image Capturing and On-Board Processing," in *IEEE Access*, vol. 7, pp. 66919-66938, 2019.

[5] Rainer Sandau, Status and trends of small satellite missions for Earth observation, Acta Astronautica, Volume 66, Issues 1–2, 2010

[6] R. N. Simons, "Applications of nano-satellites and cube-satellites in microwave and RF domain," in Proc. 2015 Int. Symp. IEEE MTT-S Microw., Phoenix, AZ, USA, Jul. 2015, pp. 1–4.

[7] Tubbal F. E., Raad R., Chin K. W., A survey and study of planar antennas for pico-satellites, IEEE Access, Dec. 2015, vol. 3, pp. 2590–2612

[8] Rahmat-Samii Y., Manohar V., Kovitz J. M., For satellites, think small, dream big: A review of recent antenna developments for CubeSats, IEEE Antennas Propag. Mag., Apr. 2017, vol. 59, no. 2, pp. 22–30

[9] J. Fouany et al., "New Concept of Telemetry X-Band Circularly Polarized Antenna Payload for CubeSat," in IEEE Antennas and Wireless Propagation Letters, vol. 16, pp. 2987-2991, 2017

[10] K. N. Khac et al., "A Design of Circularly Polarized Array Antenna for X-Band CubeSat Satellite Communication," 2018 International Conference on Advanced Technologies for Communications (ATC), Ho Chi Minh City, 2018, pp. 53-56.

[11] F. Kurniawan, J. T. S. Sumantyo, Mujtahid and A. Munir, "Effect of truncation shape against axial ratio of left-handed circularly polarized X-band antenna," 2017 15th International Conference on Quality in Research (QiR) : International Symposium on Electrical and Computer Engineering, Nusa Dua, 2017, pp. 83-86.

[12] M. A. Rahman, Q. D. Hossain, M. A. Hossain, E. Nishiyama and I. Toyoda, "Design of an x-band microstrip array antenna for circular polarization," *8th International Conference on Electrical and Computer Engineering*, Dhaka, 2014, pp. 184-187.

[13] G. Ganaraj, C. Kumar, V. S. Kumar and Shankaraiah, "High gain circularly polarized resonance cavity antenna at X-band," 2017 IEEE International Conference on Antenna Innovations & Modern Technologies for Ground, Aircraft and Satellite Applications (iAIM), Bangalore, 2017, pp. 1-5.

[14] G. V. Trentini, "Partially reflecting sheet arrays," in IRE Transactions on Antennas and Propagation, vol. 4, no. 4, pp. 666-671, October 1956.

[15] M. Asaadi and A. Sebak, "Gain and Bandwidth Enhancement of 2 × 2 Square Dense Dielectric Patch Antenna Array Using a Holey Superstrate," in IEEE Antennas and Wireless Propagation Letters, vol. 16, pp. 1808-1811, 2017.

[16] Mousavi Razi, Zahra & Rezaei, Pejman. (2013). Fabry Perot Cavity Antenna Based on Capacitive Loaded Strips Superstrate for X-Band Satellite Communication. Advanced Radar Systems Journal. 2. 26-30.

[17] Gupta, R. & Mukherjee, J.. (2010). Effect of superstrate material on a high-gain antenna using array of parasitic patches. Microwave and Optical Technology Letters. 52. 82 - 88.

[18] R. Orr, G. Goussetis and V. Fusco, "Design Method for Circularly Polarized Fabry–Perot Cavity Antennas," in *IEEE Transactions on Antennas and Propagation*, vol. 62, no. 1, pp. 19-26, Jan. 2014.

[19] L. Leszkowska, M. Rzymowski, K. Nyka, L. Kulas, Simple Superstrate Antenna for Connectivity Improvement in Precision Farming Applications, IEEE AP-S Symposium on Antennas and Propagation, 2020.